Annals of Nuclear Medicine Vol. 19, No. 8, 701–709, 2005

Evaluation of [^{11}C]SA5845 and [^{11}C]SA4503 for imaging of sigma receptors in tumors by animal PET

Kazunori KAWAMURA,*[1,2] Kazuo KUBOTA,*[3] Tadayuki KOBAYASHI,*[4] Philip H. ELSINGA,*[5] Mayumi ONO,*[6] Minoru MAEDA*[7] and Kiichi ISHIWATA*[1]

*[1]*Positron Medical Center, Tokyo Metropolitan Institute of Gerontology, Tokyo, Japan*
*[2]*SHI Accelerator Service, Tokyo, Japan*
*[3]*Department of Radiology, International Medical Center of Japan, Tokyo, Japan*
*[4]*M's Science Co., Ltd., Kobe, Japan.*
*[5]*PET-center, Groningen University Hospital, Groningen, The Netherlands*
*[6]*Department of Medical Biochemistry, Graduate School of Medical Sciences, Kyushu University, Fukuoka, Japan*
*[7]*Graduate School of Pharmaceutical Sciences, Kyushu University, Fukuoka, Japan*

Sigma receptors are expressed in a wide variety of tumor cell lines, and are expressed in proliferating cells. A radioligand for the visualization of sigma receptors could be useful for selective detection of primary tumors and their metastases, and for non-invasive assessment of tumor proliferative status. To this end we evaluated two sigma receptor ligands, [^{11}C]SA5845 and [^{11}C]SA4503. In an *in vitro* study, AH109A hepatoma showed moderate densities of $sigma_1$ and $sigma_2$ receptors, and VX-2 carcinoma showed a high density of $sigma_2$ receptors: B_{max} (fmol/mg protein) for $sigma_1$ vs. $sigma_2$, 1,700 vs. 1,200 for AH109A hepatoma and 800 vs. 10,000 for VX-2 carcinoma. In a cell growth assay *in vitro*, neither SA5845 nor SA4503 (<10 μM) showed any inhibitory effect on proliferation of the AH109A hepatoma cells. In rats, the uptake of [^{11}C]SA5845 and [^{11}C]SA4503 in AH109A tissues was accumulated over the first 60 minutes; however, the uptake of both tracers increased by co-injection with haloperidol as a sigma receptor ligand. On the other hand, in the PET studies of rabbits, the uptake of [^{11}C]SA5845 in the VX-2 carcinoma was relatively higher than that of [^{11}C]SA4503, because of a much higher density of $sigma_2$ receptors compared to $sigma_1$ receptors in the VX-2 tissue, and the uptake of both tracers in the VX-2 tissue was decreased by carrier-loading and pre-treatment with haloperidol ([^{11}C]SA5845, 53% and 26%, respectively; [^{11}C]SA4503, 41% and 22%, respectively at 30 minutes after injection). Therefore, [^{11}C]SA5845 and [^{11}C]SA4503 may be potential ligands for PET imaging of sigma receptor-rich tumors.

Key words: sigma receptor, PET, SA5845, SA4503, tumor imaging

INTRODUCTION

SIGMA RECEPTORS are widely distributed throughout the brain,[1] and are also found in endocrine, immune, and other peripheral organs.[1–4] Furthermore, sigma receptors are expressed in a variety of tumor cell lines,[5,6] and in proliferating cells.[7–9] $Sigma_2$ receptors in particular are expressed at high densities in a variety of tumor cell lines, and are increased in rapidly proliferating cells[9,10] and apoptosis.[11,12] Thus, a radioligand for the visualization of sigma receptors could be useful for the selective detection of primary tumors and their metastases, for non-invasive assessment of tumor proliferative status, and for the measurement of the sigma receptor occupancy of novel and established antineoplastic drugs. Therefore, several sigma receptor ligands have been synthesized and evaluated for positron emission tomography (PET) studies.[13–20] Furthermore, several sigma receptor ligands have cytotoxic effects on tumor cells expressing sigma receptors, suggesting antitumor agents.[11,21,22]

Received May 30, 2005, revision accepted August 24, 2005.
For reprint contact: Kazunori Kawamura, Ph.D., Positron Medical Center, Tokyo Metropolitan Institute of Gerontology, Naka-cho 1–1, Itabashi-ku, Tokyo 173–0022, JAPAN.
E-mail: kawamurak@bri.niigata-u.ac.jp.

For PET studies, we have developed ^{11}C-labeled 1-(3,4-dimethoxyphenethyl)-4-(3-phenylpropyl)piperazine ([^{11}C]SA4503)[23–27] as a sigma$_1$-selective radioligand (IC_{50}, 17 nM for sigma$_1$ and 1,800 nM for sigma$_2$),[28] and its fluorinated analog [^{11}C]1-(3,4-dimethoxyphenethyl)-4-[3-(4-fluorophenyl)propyl]piperazine ([^{11}C]SA5845)[23] as a high affinity non-subtype selective radioligand (IC_{50}, 33 nM for sigma$_1$ and 9.5 nM for sigma$_2$).[23,29] Successful imaging of the sigma$_1$ receptor in the human brain by PET with [^{11}C]SA4503[30] encouraged us to further develop [^{18}F]fluorinated analogs of SA4503 and SA5845.[23,31,32] Furthermore, 1-(4-[^{18}F]fluoroethoxy-3-methoxyphenethyl)-4-[3-(4-fluorophenyl)propyl]piperazine ([^{18}F]FE-SA5845) (IC_{50}, 3.1 nM for sigma$_1$ and 6.8 nM for sigma$_2$)[23] and [^{11}C]SA4503 were applied in a feasibility study for tumor imaging. In nude rats bearing the C6 glioma, [^{18}F]FE-SA5845 was taken up by the C6 glioma at a higher level than [^{11}C]SA4503 and the receptor-specific bindings of [^{18}F]FE-SA5845 and [^{11}C]SA4503 were 60% and 34% of the total radioactivity uptake.[33] The uptake of [^{18}F]FE-SA5845 was reduced in quiescent cells *in vitro*, in contrast to the binding of [^{11}C]SA4503.[33] This result suggests that the uptake mechanism of the non-selective sigma receptor ligand [^{18}F]FE-SA5845 in tumors is different from that of the sigma$_1$ receptor ligand [^{11}C]SA4503. Furthermore, a study with [^{11}C]SA4503 in a human volunteer indicated relatively low background in thorax and lower abdomen,[33] suggesting the potential of [^{11}C]SA4503 as a tumor imaging agent in the detection of pulmonary and abdominal tumors.

In this study, we evaluated the potential of [^{11}C]SA5845 and [^{11}C]SA4503 for tumor imaging using two different tumor models: AH109A hepatoma-bearing rats and VX-2 carcinoma-bearing rabbits. VX-2 carcinoma has a much higher density of sigma$_2$ receptors but a lower density of sigma$_1$ receptors compared to AH109A hepatoma. Also, we focused on the different mechanism of tumor uptake between a selective sigma$_1$ receptor ligand [^{11}C]SA4503 and a relatively selective sigma$_2$ receptor ligand [^{11}C]SA5845 compared with [^{18}F]FE-SA5845. Furthermore, the effect of cold ligands on proliferation of the AH109A hepatoma cells was also investigated *in vitro*, because Moody et al. suggested a relationship between tumor imaging potential and cytotoxicity.[37]

MATERIALS AND METHODS

General

1-(3,4-Dimethoxyphenethyl)-4-[3-(4-fluorophenyl)propyl]piperazine (SA5845), 1-(3,4-dimethoxyphenethyl)-4-(3-phenylpropyl)piperazine (SA4503) and (+)-pentazocine were prepared by Santen Pharmaceutical Co. Ltd. (Osaka, Japan). Haloperidol (Serenace^R) was purchased from Dainippon Pharmaceutical Co. Ltd. (Osaka, Japan). [^{3}H](+)-Pentazocine (1.04 TBq/mmol) and [^{3}H]1,3-di-*o*-tolylguanidine ([^{3}H]DTG, 1.11 TBq/mmol) were purchased from NEN^{TM} Life Science Products (Boston, MA).

[^{11}C]SA5845 and [^{11}C]SA4503 were prepared by methylation of the respective 4-*O*-demethyl compound with [^{11}C]methyl iodide as previously described.[23,24] The specific activity of [^{11}C]SA5845 and [^{11}C]SA4503 was 55–298 TBq/mmol at end-of-bombardment.

Male Donryu rats (8–9 weeks old, 200–307 g) and female Japanese white rabbits bearing VX-2 carcinoma (shope papilloma) on the thigh (13–16 weeks old, 2.0–2.7 kg) were purchased from Tokyo Laboratory Animals Co. Ltd. (Tokyo, Japan). The rats bearing AH109A hepatoma were prepared by subcutaneous inoculation of 0.1 m*l* suspension of AH109A ascitic hepatoma cells (approximately 10^7 cells) in the thigh.[34] The rats were used for the following experiments 7–10 days after inoculation. The animal studies were approved by the Animal Care and Use Committee of the Tokyo Metropolitan Institute of Gerontology.

In vitro *measurement of sigma$_1$ and sigma$_2$ receptors in tumor tissues*

Sigma$_1$ and sigma$_2$ receptors in the AH109A hepatoma or VX-2 carcinoma tissues were measured by membrane binding assays. The tumors were removed from the rats and rabbits and homogenized in eight volumes (w/v) of ice-cold 50 mmol/*l* Tris-HCl buffer (pH 7.7 at 25°C) containing 0.32 mol/*l* sucrose with a teflon-glass homogenizer. The homogenates were centrifuged at 1,000 × *g* for or 10 minutes at 4°C, and the supernatant was collected and centrifuged at 47,000 × *g* for 20 minutes at 4°C. The resulting membrane pellets were re-suspended with 20 volumes (w/v) of ice-cold 50 mmol/*l* Tris-HCl buffer (pH 7.7 at 25°C) containing 0.32 mol/*l* sucrose. Sigma$_1$ and sigma$_2$ receptor binding assays were performed by the methods previously described.[23,28] Radioligands used for the binding assay were [^{3}H](+)-pentazocine for the sigma$_1$ receptors and [^{3}H]DTG in the presence of 100 nmol/*l* (+)-pentazocine for the sigma$_2$ receptors. Incubations were carried out in triplicate at 37°C for 150 minutes in the binding study with [^{3}H](+)-pentazocine, and at 25°C for 90 minutes in the study with [^{3}H]DTG.

K_d and B_{max} values were determined using the computerized interactive curve-fitting program GraphPad Prism® version 3.0c for Macintosh (GraphPad Software, San Diego, CA).

AH109A hepatoma cell growth inhibition assay

CellTiter-Glo Luminescent Cell Viability Assay Kit (Promega, Madison, WI) was used to determine the effect of SA5845 and SA4503 on cell proliferation in the AH109A hepatoma cells. One hundred microliters of an exponentially growing cell suspension (2×10^3 cells) was seeded into a 96-well plate. The following day, various concentrations (0, 1, 5 and 10 μM) of SA5845 or SA4503 were added. After incubation for 72 h at 37°C, 100 μ*l* of

Table 1 Binding parameters of $sigma_1$ and $sigma_2$ receptor in the AH109A hepatoma and VX-2 carcinoma

	$Sigma_1$ receptor*		$Sigma_2$ receptor#	
	K_d (nM)	B_{max} (fmol/mg protein)	K_d (nM)	B_{max} (fmol/mg protein)
AH109A	86 ± 18	1,700 ± 240	23 ± 1.9	1,200 ± 46
VX-2	45 ± 20	810 ± 210	27 ± 2.0	10,000 ± 370

Values are the average of 3 experiments ± S.D.
*Membranes were incubated using [^{3}H](+)-pentazocine for 90 minutes at 25°C.
#Membranes were incubated using [^{3}H]DTG for 150 minutes at 37°C in the presence of (+)-pentazocine to mask $sigma_1$ receptors.

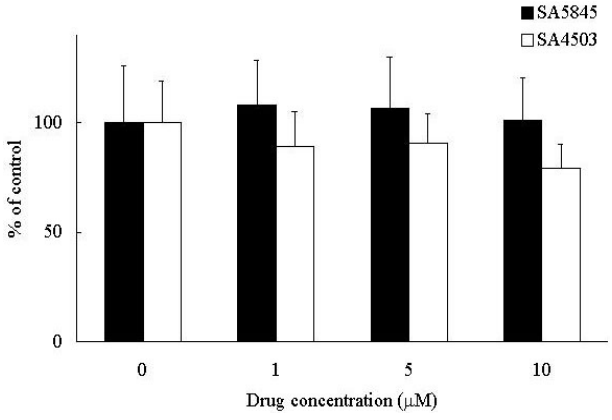

Fig. 1 The effect of SA5845 and SA4503 on proliferation of AH109A hepatoma cells *in vitro*. Cell densities were evaluated in triplicate by a luminescent assay, and expressed as a percentage of the control (average ± S.D.).

CellTier-Glo Reagent was added to each well and the plates were shaken gently for 2 minutes. After incubation for 10 min at room temperature, luminescence was measured using a multilabel counter (Wallac, Tokyo, Japan).[35] Each experiment was done using three replicate wells for each drug concentration.

Tissue distribution in AH109A hepatoma-bearing rats
[^{11}C]SA5845 (11 MBq/0.30 nmol) or [^{11}C]SA4503 (17 MBq/0.29 nmol) was intravenously injected into rats bearing the AH109A hepatoma. The rats were sacrificed by cervical dislocation at 5, 15, 30 and 60 minutes after injection (n = 5). The blood was collected by heart puncture, and the brain, lung, liver, spleen, kidney, muscle and AH109A tissues were harvested and weighed. The radioactivity of ^{11}C in the samples was measured with a gamma scintillation counter. The tissue uptake of ^{11}C was expressed as the percentage of the injected dose per gram of tissue (%ID/g).

To determine receptor-specific uptakes, the non-subtype selective sigma receptor ligand haloperidol was used as a blocking agent. [^{11}C]SA5845 (11 MBq/0.30 nmol) or [^{11}C]SA4503 (10 MBq/0.53 nmol) was co-injected with haloperidol (1 mg/kg), and 30 minutes later rats were sacrificed by cervical dislocation (n = 5). The tissue uptake was measured as %ID/g as described above.

Metabolite analysis in AH109A hepatoma-bearing rats
[^{11}C]SA5845 (85–98 MBq/1.2–1.3 nmol) or [^{11}C]SA4503 (140–170 MBq/1.7–2.0 nmol) was intravenously injected into rats, and 30 minutes later rats were sacrificed by cervical dislocation. Blood was removed by heart puncture using a heparinized syringe, and AH109A tissue was harvested. The blood was centrifuged at 7,000 × *g* for 1 minute at 4°C to obtain plasma, which was then treated with acid-deproteinization as previously described.[23] The AH109A tissue was homogenized in 1 m*l* of 20% trichloroacetic acid in acetonitrile/water (1/1, v/v). The homogenate was then treated with the same acid-deproteinization method as the plasma. The combined supernatant was analyzed by high-performance liquid chromatography with a radioactivity detector (FLO-ONE/Beta A200, Packard, Meriden, CT). A Radial-Pak C18 column equipped in an RCM 8 × 10 module (8 mm × 100 mm, Waters, Milford, MA) was used with a mixture of acetonitrile and 50 mmol/*l* sodium acetate buffer (pH 6.0) (40/60, v/v) at a flow rate of 2 m//minute.

PET measurement
PET measurement was performed in two rats bearing the AH109A hepatoma and four rabbits bearing the VX-2 carcinoma with a model SHR-2000 PET camera (Hamamatsu Photonics K.K., Hamamatsu, Japan) as previously described.[36] The camera provides a set of 7-slice images at center-to-center intervals of 6.5 mm with an image spatial resolution of 4.0 mm full width at half maximum, and an axial resolution of 5.0 mm full width at half maximum.

Each rat was anesthetized with isoflurane (2.0%) and was fixed in a prone position on the bed of the camera. After a transmission scan to correct for attenuation, [^{11}C]SA5845 (14 MBq/1.28 nmol) or [^{11}C]SA4503 (19 MBq/0.12 nmol) was intravenously injected into the rats, and a time-sequential tomographic scan was performed for 60 minutes (60 frames per 60 minutes). Forty-five minutes after the first PET scan, the rats were treated by intravenous injection of haloperidol (1 mg/kg), then 15 or 20 minutes later [^{11}C]SA5845 (15 MBq/0.45 nmol) or [^{11}C]SA4503 (20 MBq/0.33 nmol) was injected, and a

Table 2 Tissue distribution of radioactivity after intravenous injection of [^{11}C]SA5845 in rats bearing the AH109A hepatoma

	Uptake (%ID/g)*			
	5 min	15 min	30 min	60 min
Brain	0.94 ± 0.12	0.88 ± 0.29	0.89 ± 0.04	0.98 ± 0.07
Lung	4.25 ± 0.52	2.69 ± 0.17	1.85 ± 0.42	1.49 ± 0.21
Liver	0.73 ± 0.31	1.11 ± 0.29	1.45 ± 0.54	1.63 ± 0.20
Spleen	0.84 ± 0.27	0.90 ± 0.10	1.02 ± 0.25	0.95 ± 0.08
Kidney	2.45 ± 0.75	2.26 ± 0.25	2.43 ± 0.45	2.29 ± 0.21
Muscle	0.40 ± 0.12	0.35 ± 0.10	0.28 ± 0.05	0.23 ± 0.03
Blood	0.09 ± 0.01	0.06 ± 0.004	0.04 ± 0.01	0.03 ± 0.01
Tumor	0.24 ± 0.08	0.26 ± 0.06	0.37 ± 0.04	0.49 ± 0.05

*Uptake values are represented as mean percentage of the injection dose per gram of tissue (%ID/g) ± S.D. (n = 5).

Table 3 Tissue distribution of radioactivity after intravenous injection of [^{11}C]SA4503 in rats bearing the AH109A hepatoma

	Uptake (%ID/g)*			
	5 min	15 min	30 min	60 min
Brain	0.99 ± 0.12	0.92 ± 0.07	0.87 ± 0.07	0.69 ± 0.15
Lung	3.17 ± 0.88	1.60 ± 0.29	1.08 ± 0.18	0.70 ± 0.15
Liver	3.84 ± 0.62	4.00 ± 1.39	5.35 ± 2.21	5.73 ± 1.34
Spleen	0.92 ± 0.12	1.05 ± 0.10	1.13 ± 0.13	0.81 ± 0.18
Kidney	3.33 ± 0.21	2.89 ± 0.28	2.52 ± 0.17	1.78 ± 0.18
Muscle	0.30 ± 0.04	0.22 ± 0.04	0.16 ± 0.02	0.11 ± 0.04
Blood	0.17 ± 0.01	0.07 ± 0.01	0.07 ± 0.02	0.05 ± 0.01
Tumor	0.30 ± 0.08	0.50 ± 0.17	0.60 ± 0.23	0.67 ± 0.19

*Uptake values are represented as mean percentage of the injection dose per gram of tissue (%ID/g) ± S.D. (n = 5).

Table 4 Effects of co-injection of haloperidol on tissue radioactivity at 30 minutes after intravenous injection of [^{11}C]SA5845 or [^{11}C]SA4503 into rats bearing the AH109A hepatoma

	[^{11}C]SA5845		[^{11}C]SA4503	
	Control	Haloperidol	Control	Haloperidol
Brain	0.89 ± 0.04	0.34 ± 0.03*	0.86 ± 0.08	0.31 ± 0.02*
Lung	1.85 ± 0.42	1.15 ± 0.49*	1.27 ± 0.21	0.83 ± 0.08*
Liver	1.45 ± 0.54	1.81 ± 0.20	3.11 ± 0.84	3.08 ± 0.18
Spleen	1.02 ± 0.25	1.03 ± 0.14	0.91 ± 0.09	0.89 ± 0.15
Kidney	2.43 ± 0.45	0.86 ± 0.09*	2.52 ± 0.36	0.84 ± 0.03*
Muscle	0.28 ± 0.05	0.17 ± 0.04*	0.23 ± 0.04	0.17 ± 0.02*
Blood	0.04 ± 0.01	0.11 ± 0.01*	0.05 ± 0.01	0.16 ± 0.01*
Tumor	0.37 ± 0.04	0.60 ± 0.15*	0.44 ± 0.17	0.74 ± 0.13*
T/B[#]	9.7	5.6	8.8	4.7
T/M[$]	1.3	3.5	1.9	4.5

Uptake values are represented as mean percentage of the injection dose per gram of tissue (%ID/g) ± S.D. (n = 5). *$p < 0.05$ (Student's t-test, compared with control).

[#]The uptake ratio of tumor to blood.

[$]The uptake ratio of tumor to muscle.

second 60-minute PET scan was performed.

In the rabbits, four PET scans were successively performed in the same day: two baseline scans for each tracer followed by the other two scans in the haloperidol-blockade. The rabbits were anesthetized with isoflurane (1.5–2.0%) and were fixed in a semi-prone position on the bed of the camera. After a transmission scan, [^{11}C]SA4503 (26 MBq/0.28 nmol) was intravenously injected, and a

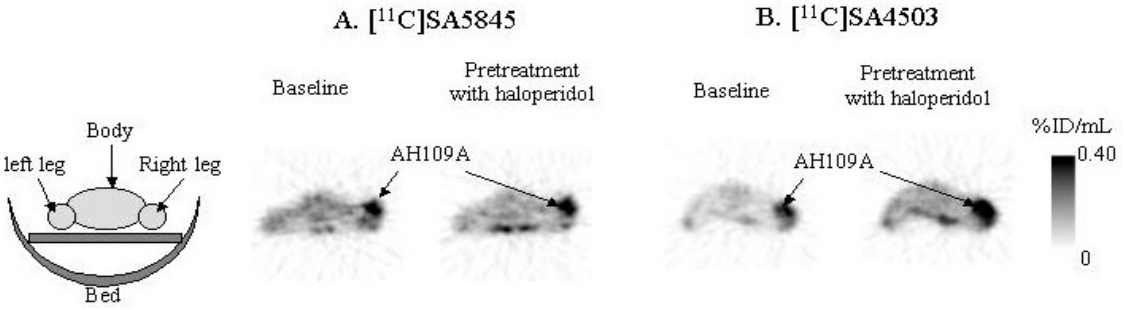

Fig. 2 Images of AH109A hepatoma-bearing rats by PET with [^{11}C]SA5845 (A) and [^{11}C]SA4503 (B) in the baseline and haloperidol-pretreatment (1 mg/kg) condition. Two PET scans in (A) or (B) were performed in the same individual rat. The rat was fixed in a prone position on the bed of the camera. The PET images were acquired for 20 minutes starting at 40 minutes after injection.

time-sequential tomographic scan was performed for 60 minutes (60 frames per minute). Sixty minutes later, the second 60-minute PET scan with [^{11}C]SA5845 (86 MBq/0.78 nmol) was performed. Forty-five minutes after the second 60-minute PET scan, haloperidol (1 mg/kg) was intravenously injected, and 15 minutes later the third 60-minute PET scan with [^{11}C]SA4503 (94 MBq/0.87 nmol) was performed. Sixty minutes after the third scan, the fourth 60-minute PET with [^{11}C]SA5845 (97 MBq/1.1 nmol) scan was performed.

In each of the other two rabbits, two PET scans were successively performed in baseline scan and carrier-loading conditions. After a transmission scan, a 60-minute PET scan with [^{11}C]SA5845 (106 MBq/5.7 nmol) or [^{11}C]SA4503 (117 MBq/2.4 nmol) was performed. Sixty minutes later, [^{11}C]SA5845 (98 MBq/3.9 nmol) or [^{11}C]SA4503 (108 MBq/2.2 nmol) was intravenously co-injected with cold SA5845 (1 mg/kg) or cold SA4503 (1 mg/kg), and a second 60-minute PET scan was performed.

To measure the time-activity curves, the regions of interest (ROIs) were placed on the AH109A and VX-2 tissues, and muscle based on PET images. The location of the tissues was confirmed by tissue dissection after the PET measurement. The decay-corrected radioactivity values were expressed as a percentage of the injected dose per m*l* of tissue volume (%ID/m*l*).

RESULTS

In vitro *measurement of sigma$_1$ and sigma$_2$ receptors in tumor tissues*

Table 1 summarizes the sigma$_1$ and sigma$_2$ receptor densities in the AH109A hepatoma and VX-2 carcinoma as determined in our experiments. The AH109A hepatoma was found to express a moderate density of two sigma receptor subtypes. In the VX-2 carcinoma the density of sigma$_2$ receptors (10,000 fmol/mg protein) was over ten-fold that of sigma$_1$ receptors (810 fmol/mg protein), and eight-fold that of sigma$_2$ receptors in the AH109A hepatoma (1,200 fmol/mg protein). The K_d values for sigma$_2$ receptors were smaller than those for sigma$_1$ receptors in both the AH109A hepatoma and VX-2 carcinoma.

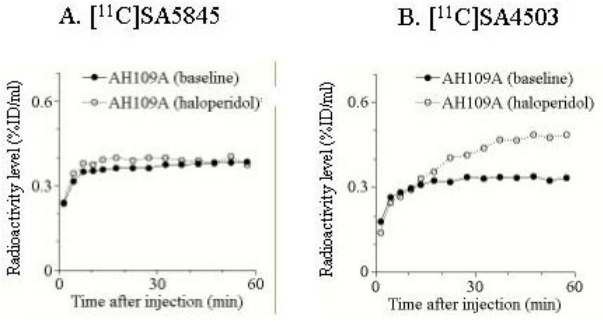

Fig. 3 Time-radioactivity curves of the AH109A hepatoma after intravenous injection of [^{11}C]SA5845 (A) or [^{11}C]SA4503 (B) in the baseline and haloperidol-pretreatment (1 mg/kg) condition (n = 1). Two PET scans in (A) or (B) were performed in the same individual rat.

AH109A hepatoma cell growth inhibition assay

The effects of SA5845 and SA4503 on proliferation of AH109A hepatoma cells are summarized in Figure 1. There are no significant difference between control and less than 10 μM SA5845 and SA4503. SA4503 showed a little tendency of growth inhibition.

Tissue distribution in AH109A hepatoma-bearing rats

The tissue distribution of radioactivity after injection of [^{11}C]SA5845 and [^{11}C]SA4503 into rats bearing the AH109A hepatoma is summarized in Tables 2 and 3, respectively. Both tracers showed similar distribution patterns in the lung, spleen, blood and AH109A tissue. In the brain, the uptake of [^{11}C]SA4503 decreased over 60 minutes; however, that of [^{11}C]SA5845 increased or remained constant from 15 to 60 minutes. In the kidney, the uptake of [^{11}C]SA4503 decreased over 60 minutes; however, that of [^{11}C]SA5845 remained at a high level over 60

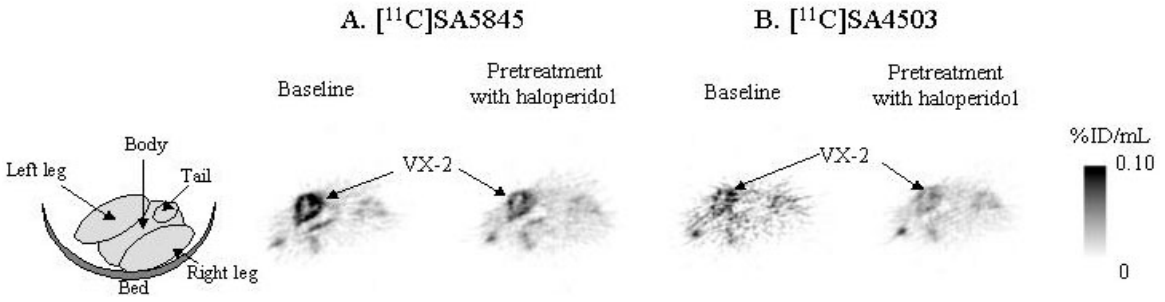

Fig. 4 Images of VX-2 carcinoma-bearing rabbits by PET with [^{11}C]SA5845 (A) and [^{11}C]SA4503 (B) in the baseline and haloperidol-pretreatment (1 mg/kg) condition. PET scans were performed in the same rabbit. The rabbit was fixed in a semi-prone position on the bed of the camera. The PET images were acquired for 20 minutes starting at 40 minutes after injection.

minutes. In the liver, the uptake of [^{11}C]SA4503 was much higher than the uptake of [^{11}C]SA5845 over 60 minutes. The tracers uptake increased in the AH109A tissue and liver over the first 60 minutes, while uptake levels decreased in the lung, muscle, and blood from 5 to 60 minutes.

The effects of co-injection with haloperidol on the tissue distribution of radioactivity 30 minutes after the intravenous injection of [^{11}C]SA5845 or [^{11}C]SA4503 into rats bearing the AH109A hepatoma are summarized in Table 4. After co-injection with haloperidol, the radioactivity levels of both tracers significantly decreased in the brain, kidney, and muscle. However, the radioactivity levels of the tracers in the AH109A tissue and blood were significantly increased by the haloperidol treatment. The AH109A-to-blood ratios significantly decreased; however, the AH109A-to-muscle ratios increased.

Metabolite analysis in AH109A hepatoma-bearing rats

Metabolite analysis was carried out in AH109A tissues and plasma 30 minutes after injection. The recovery of the radioactivity in the HPLC analysis was essentially quantitative. Percentages of unchanged [^{11}C]SA5845 and [^{11}C]SA4503 were 95.4 ± 1.9% and 90.3 ± 2.6% (n = 3), respectively, in AH109A tissue and 75.1 ± 7.9% and 81.0 ± 2.7% (n = 3), respectively, in plasma.

PET measurement

Figure 2 shows PET images of the AH109A hepatoma on the thigh with [^{11}C]SA5845 and [^{11}C]SA4503 in rats fixed in a prone position on the bed. Both tracers showed a high uptake in the AH109A tissue; however, uptake in the AH109A tissue could not be blocked by pretreatment with haloperidol, as shown in the time-activity curves (Fig. 3).

Figure 4 shows PET images of the VX-2 carcinoma on the thigh with [^{11}C]SA5845 and [^{11}C]SA4503 in rabbits fixed in a semi-prone position on the bed. PET with each of the two tracers clearly visualized VX-2 tissue, and uptake of [^{11}C]SA5845 in the VX-2 tissue was higher than that of [^{11}C]SA4503. However, PET images with each of the two tracers on the central regions of the VX-2 tissues were not well visualized because the central regions of the VX-2 tissues were necrotic. The pretreatment with haloperidol clearly decreased the uptake of each of the two tracers in the VX-2 tissue.

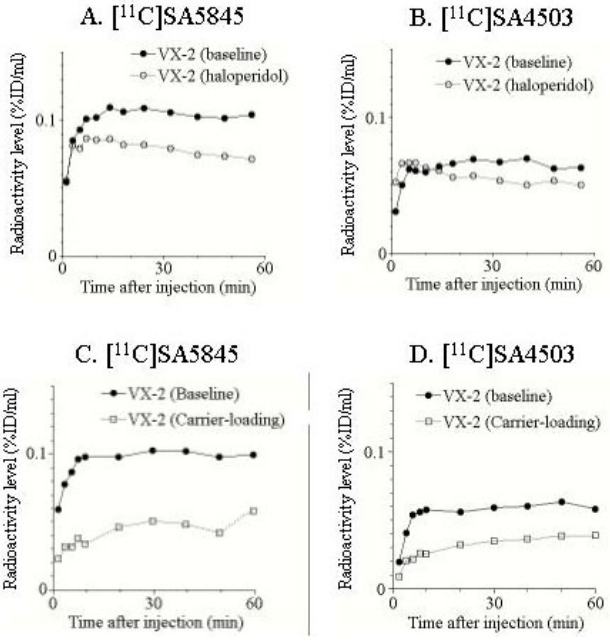

Fig. 5 Time-radioactivity curves of the VX-2 carcinoma after intravenous injection of [^{11}C]SA5845 (A) or [^{11}C]SA4503 (B) in the baseline and haloperidol-pretreatment (1 mg/kg) condition, and after intravenous injection of [^{11}C]SA5845 (C) or [^{11}C]SA4503 (D) in the baseline and carrier-loading (1 mg/kg) condition. Four PET scans in (A) and (B) were performed in the same rabbit and two PET scans in (C) or (D) were performed in each of the two other rabbits.

Figure 5 shows time-radioactivity curves for the VX-2 tissue of the rabbits. The radioactivity level of both tracers in the VX-2 tissue increased for the first 10 minutes and remained constant in the baseline measurement. The uptake level of [^{11}C]SA5845 in the VX-2 carcinoma was

Table 5 Specific binding of [^{11}C]SA5845, [^{11}C]SA4503, [^{18}F]FE-SA5845 and 2-[^{18}F]FBP in various tumors

Tracer	Tumor (animal)	Sigma receptor density B_{max} (fmol/mg protein)	Specific binding (%)		Ref.
			Haloperidol	Carrier-loading	
[^{11}C]SA5845	VX-2 carcinoma (rabbit)	11,000	26* (n = 2)	53* (n = 1)	
[^{11}C]SA4503			22* (n = 1)	41* (n = 1)	
[^{11}C]SA4503	C6 glioma (rat)	11,000$^{\$}$	34$^{\#}$ (n = 3)		[33]
[^{18}F]FE-SA5845			60$^{\#}$ (n = 5)		[33]
2-[^{18}F]FBP	Human breast adenocarcinoma (mouse)	9,100†	44$^{\#}$ (n = 2)		[41]

*Mean values acquired from 25 to 35 minutes after injection of the tracer; $^{\#}$Values are represented as mean values at 60 minutes after injection of the tracer; $^{\$}$ref. [40]; †Ref. [42].

relatively higher than that of [^{11}C]SA4503. In the haloperidol-pretreatment condition, the initial uptake of [^{11}C]SA5845, but not [^{11}C]SA4503, in the VX-2 tissue was slightly lower than that in the baseline and the radioactivity levels of both tracers decreased with time. In contrast to the haloperidol-pretreatment, carrier-loading showed much larger blocking effects for both tracers (Table 5).

DISCUSSION

Sigma receptors are expressed in a wide variety of tumor cell lines,[5,6] and generally the densities of sigma$_2$ receptors are higher than those of sigma$_1$ receptors.[6] Therefore, high affinity sigma$_2$ receptor radioligands are particularly useful for the imaging of tumors by PET or SPECT. In this study, we found that both sigma$_1$ and sigma$_2$ receptor subtypes are expressed in the AH109A hepatoma and VX-2 carcinoma implanted in rats and rabbits, respectively. The density of sigma$_2$ receptors in the VX-2 carcinoma was much higher than that of sigma$_1$ receptors, and also much higher than that of sigma$_2$ receptors in the AH109A hepatoma. In AH109A hepatoma cells *in vitro*, little growth inhibition was observed using 1 or 5 or 10 μM SA5845 and SA4503, although there was a tendency to dose-dependent growth inhibition with the use of less than 10 μM SA4503. Recently, in the tumor cell growth studies of sigma receptor ligands, *N*-(2-(piperidino)ethyl)-2-iodobenzamide (2-IBP) and (2-piperidinyl-aminoethyl)-4-iodobenzamide (IPAB), little growth inhibition was observed using 0.1 or 1 μM IPAB, whereas proliferation was inhibited by 50% using 10 μM IPAB or 20 μM 2-IPB in NCI-N417 small cell lung cancer cells.[37] Furthermore, treatment with 10 μM haloperidol or 10 μM DTG reduced colony formation by approximately 90% in NCI-N417 small cell lung cancer cells.[37] Therefore, SA4503 and SA5845 may have a much less inhibitory effect on proliferation of tumor cells than other sigma receptor ligands such as 2-IBP, IPAB, haloperidol and DTG, although the tumor cell lines investigated were not the same.

In the AH109A hepatoma inoculated rats *in vivo*, both [^{11}C]SA5845 and [^{11}C]SA4503 increased over 60 minutes after injection; however, no blocking effects were found by the haloperidol-pretreatment. Instead, an enhanced uptake of both tracers was found in the AH109A hepatoma. A possible explanation may be the blocking of binding sites in normal organs by haloperidol as shown in the brain, kidney and lung, together with the relatively lower densities of sigma receptors in the AH109A hepatoma than in other tumors, as discussed later. On the other hand, clear specific binding was found in the brain, whereas the receptor densities in the brain (sigma$_1$ receptors, 74–200 fmol/mg protein; sigma$_2$ receptors, 110–300 fmol/mg protein)[38] were lower than that in the AH109A hepatoma. In the present study, the radioactivity level of blood increased by about 3 fold, which resulted in an increased influx of radioligands from the blood to the AH109A hepatoma. Therefore, the absence of any blocking effect of haloperidol in the AH109A hepatoma may be explained by interference from an increased influx of radioligands from the blood, because the blood fraction in the tumor was generally higher than that in the brain. At 30 minutes after the injection of both tracers, a high percentage of the radioligands was still in the form of their parent compounds ([^{11}C]SA5845, 95%; [^{11}C]SA4503, 90%) in the AH109A tissue. Therefore, it is suggested that the increased uptake of both tracers by treatment with haloperidol may not be related to the uptake of metabolites. Regarding tumor imaging potential of sigma receptor radioligands, a similar result was also observed in the study of another sigma$_1$-selective radioligand [^{18}F]1-(3-fluoropropyl)-4-(4-cyanophenoxymethyl)piperidine using a different animal model,[39] suggesting that the tumor uptake of these tracers could be due to factors other than the binding of sigma receptors.

In the VX-2 carcinoma, the uptake of [^{11}C]SA5845 was higher than that of [^{11}C]SA4503, and the receptor-specific binding of [^{11}C]SA5845 was also higher than that of [^{11}C]SA4503: 26% vs. 22% in the haloperidol-treatment and 53% vs. 41% in the carrier-loading measurement. Because the VX-2 carcinoma has a much higher density of sigma$_2$ receptors compared with sigma$_1$ receptors, these differences are mainly due to the higher affinity of [^{11}C]SA5845 for sigma$_2$ receptors compared with

[^{11}C]SA4503. It is noted that the blocking effects of haloperidol and carrier-loading were different, although, both treatments showed similar blocking effects in the rat brain.[23] The findings suggest that there are tracer-specific binding sites in the VX-2 tissue and/or unknown mechanisms of tracer accumulation.

The different results between the AH109A hepatoma and VX-2 carcinoma may be explained by a difference in the density of sigma receptors. The VX-2 carcinoma has a much higher density of sigma$_2$ receptors than the AH109A hepatoma. Recently, we demonstrated specific-binding of [^{11}C]SA4503 and [^{18}F]FE-SA5845 to sigma receptors in the C6 rat glioma.[33] The percentage of receptor specific binding of [^{11}C]SA4503 and [^{18}F]FE-SA5845 in the haloperidol-treatment was 34% and 60%, respectively (Table 5). The sigma receptor density of the C6 rat glioma (B_{max} = 11,000 fmol/mg protein)[40] was higher than that of the AH109A hepatoma (B_{max} = 1,700 and 1,200 fmol/mg protein for the sigma$_1$ and sigma$_2$ binding sites, respectively). Therefore, it is considered that *in vivo* specific binding for sigma receptors is relatively higher in sigma receptor-rich tumors and less masked by the effect of an increased influx of blood to tumor. In the case of another sigma$_1$-selective receptor radioligand, *N*-(*N*-benzylpiperidin-4-yl)-2-[^{18}F]fluorobenzamide (2-[^{18}F]FBP),[41] the uptake of 2-[^{18}F]FBP in human breast tumor decreased after pretreatment with haloperidol at 60 and 120 minutes after injection of 2-[^{18}F]FBP into mice. The sigma receptor density of the human breast tumor (B_{max} = 9,000 fmol/mg protein)[42] was also higher than that of the AH109A hepatoma. However, the specific binding of [^{11}C]SA5845 and [^{11}C]SA4503 in the VX-2 carcinoma was lower than that of [^{11}C]SA4503 and [^{18}F]FE-SA5845 in the C6 rat glioma or that of 2-[^{18}F]FBP in the human breast tumor (Table 5). The different results may be explained by the affinity of the radioligand for the sigma receptors. FE-SA5845 (IC_{50} for sigma$_1$, 3.1 nM; IC_{50} for sigma$_2$, 6.8 nM)[23] and 2-FBP (K_i for sigma$_1$, 3.4 nM; K_i for sigma$_2$, 406 nM)[16] have a higher affinity for the sigma receptor than SA5845 (IC_{50} for sigma$_1$, 33 nM; IC_{50} for sigma$_2$, 9.5 nM)[23] and SA4503 (IC_{50} for sigma$_1$, 17 nM; IC_{50} for sigma$_2$, 1,800 nM).[28] On the other hand, the specific binding of [^{11}C]SA4503 in the VX-2 carcinoma was lower than that in the C6 glioma. This effect may be explained by species differences between rabbits with the VX-2 carcinoma and rats with the C6 glioma.

In conclusion, [^{11}C]SA5845 and [^{11}C]SA4503 may be potential ligands for PET imaging of sigma receptor-rich tumors. However, [^{11}C]SA5845 and [^{11}C]SA4503 may be inferior to [^{18}F]FE-SA5845 or 2-[^{18}F]FBP. The exact mechanism of tumor uptake is still unclear, as shown in the AH109A hepatoma, and needs further investigation.

ACKNOWLEDGMENT

This work was supported by a Grant-in-Aid for Scientific Research (B) No. 13557077 of Japan Society for the Promotion of Science.

REFERENCES

1. Walker JM, Bowen WD, Walker FO, Matsumoto RR, de Costa B, Rice KC. Sigma receptors: biology and function. *Pharmacol Rev* 1990; 42: 355–402.
2. Su TP, London ED, Jaffe JH. Steroid binding at σ receptors suggests a link between endocrine, nervous, immune systems. *Science* 1988; 240: 219–221.
3. Wolfe SA Jr, Culp SG, De Souza EB. σ-receptors in endocrine organs: identification, characterization, and autoradiogaphic localization on rat pituitary, adrenal, testis and ovary. *Endocrinology* 1989; 124: 1160–1172.
4. Hellewell SB, Bruce A, Feinstein G, Orringer J, Williams W, Bowen WD. Rat liver and kidney contain high densities of σ_1 and σ_2 receptors: characterization by ligand binding and photoaffinity labeling. *Eur J Pharmacol* 1994; 268: 9–18.
5. Bem WT, Thomas GE, Mamone JY, Homan SM, Levy BK, Johnson FE, et al. Overexpression of σ receptors in nonneural human tumors. *Cancer Res* 1991; 51: 6558–6562.
6. Vilner BJ, John CS, Bowen WD. Sigma-1 and sigma-2 receptors are expressed in a wide variety of human and rodent tumor cell lines. *Cancer Res* 1995; 55: 408–413.
7. Brent PJ, Pang GT. σ binding site ligands inhibit cell proliferation in a mammary and colon carcinoma cell lines and melanoma cells in culture. *Eur J Pharmacol* 1995; 278: 151–160.
8. Wheeler KT, Wang LM, Wallen CA, Childers SR, Cline JM, Keng PC, et al. Sigma-2 receptors as a biomarker of proliferation in solid tumours. *Br J Cancer* 2000; 82: 1223–1232.
9. Mach RH, Smith CR, Al Nabulsi I, Whirrett BR, Childers SR, Wheeler KT. Sigma-2 receptors as potential biomarkers of proliferation in breast cancer. *Cancer Res* 1997; 57: 156–161.
10. Zamora PO, Moody TW, John CS. Increased binding to sigma sites of *N*-[1′(2-piperidinyl)ethyl]-4-[I-125]-iodobenzamide (I-125-PAB) with onset of tumor cell proliferation. *Life Sci* 1998; 63: 1611–1618.
11. Crawford KW, Bowen WD. Sigma-2 receptor agonists activate a novel apoptotic pathway and potentiate antineoplastic drugs in breast tumor cell lines. *Cancer Res* 2002; 62: 313–322.
12. Crawford KW, Coop A, Bowen WD. σ_2 Receptors regulate changes in sphingolipid levels in breast tumor cells. *Eur J Pharmacol* 2002; 443: 207–209.
13. Wilson AA, Dannals RF, Ravert HT, Sonders MS, Weber E, Wagner HN Jr. Radiosynthesis of sigma receptor ligands for positron emission tomography: ^{11}C- and ^{18}F-labeled guanidines. *J Med Chem* 1991; 34: 1867–1870.
14. Musachio JL, Scheffel U, Stathis M, Ravert HT, Mathews WB, Dannals RF. (+)-[C-11]-*cis*-*N*-benzyl-normetazocine: a selective ligand for sigma receptors *in vivo*. *Life Sci* 1994; 55: PL225–232.
15. Dence CS, John CS, Bowen WD, Welch MJ. Synthesis and evaluation of [^{18}F] labeled benzamides: High affinity sigma receptor ligands for PET imaging. *Nucl Med Biol* 1997; 24: 333–340.

16. Shiue CY, Shiue GG, Zhang SX, Wilder S, Greenberg JH, Benard F, et al. *N*-(*N*-Benzylpiperidin-4-yl)-2-[^{18}F]fluorobenzamide: a potential ligand for PET imaging of sigma receptors. *Nucl Med Biol* 1997; 24: 671–676.
17. Waterhouse RN, Collier TL. *In vivo* evaluation of [^{18}F]1-(3-fluoropropyl)-4-(4-cyanophenoxymethyl)piperidine: a selective sigma-1 receptor radioligand for PET. *Nucl Med Biol* 1997; 24: 127–134.
18. Ishiwata K, Noguchi J, Ishii S, Hatano K, Ito K, Nabeshima T, et al. Synthesis of [^{11}C]NE-100 labeled in two different positions as a PET σ receptor ligand. *Nucl Med Biol* 1998; 25: 195–202.
19. Kawamura K, Ishiwata K, Tajima H, Ishii S, Shimada Y, Matsuno K, et al. Synthesis and *in vivo* evaluation of [^{11}C]SA6298 as a PET sigma$_1$ receptor ligand. *Nucl Med Biol* 1999; 26: 915–922.
20. Mach RH, Huang Y, Buchheimer N, Kuhner R, Wu L, Morton TE, et al. [^{18}F]*N*-(4′-fluorobenzyl)-4-(3-bromophenyl) acetamide for imaging the sigma receptor status of tumors: comparison with [^{18}F]FDG, and [^{125}I]IUDR. *Nucl Med Biol* 2001; 28: 451–458.
21. Barbieri F, Sparatore A, Alama A, Novelli F, Bruzzo C, Sparatore F. Novel sigma binding site ligands as inhibitors of cell proliferation in breast cancer. *Oncol Res* 2003; 13: 455–461.
22. Casellas P, Galiegue S, Bourrie B, Ferrini JB, Jbilo O, Vidal H. SR31747A: a peripheral sigma ligand with potent antitumor activities. *Anticancer Drugs* 2004; 15: 113–118.
23. Kawamura K, Elsinga PH, Kobayashi T, Ishii S, Wang WF, Matsuno K, et al. Synthesis and evaluation of ^{11}C- and ^{18}F-labeled 1-[2-(4-alkoxy-3-methoxyphenyl)ethyl]-4-(3-phenylpropyl)piperazines as sigma receptor ligands for positron emission tomography studies. *Nucl Med Biol* 2003; 30: 273–284.
24. Kawamura K, Ishiwata K, Tajima H, Ishii S, Matsuno K, Homma Y, et al. *In vivo* evaluation of [^{11}C]SA4503 as a PET ligand for mapping CNS sigma$_1$ receptors. *Nucl Med Biol* 2000; 27: 255–261.
25. Kawamura K, Ishiwata K, Shimada Y, Kimura Y, Kobayashi T, Matsuno K, et al. Preclinical evaluation of [^{11}C]SA4503: radiation dosimetry, *in vivo* selectivity and PET imaging of sigma$_1$ receptors in the cat brain. *Ann Nucl Med* 2000; 14: 285–292.
26. Kawamura K, Kimura Y, Tsukada H, Kobayashi T, Nishiyama S, Kakiuchi T, et al. An increase of sigma receptors in the aged monkey brain. *Neurobiol Aging* 2003; 24: 745–752.
27. Ishiwata K, Tsukada H, Kawamura K, Kimura Y, Nishiyama S, Kobayashi T, et al. Mapping of CNS sigma$_1$ receptors in the conscious monkey: Preliminary PET study with [^{11}C]SA4503. *Synapse* 2001; 40: 235–237.
28. Matsuno K, Nakazawa M, Okamoto K, Kawashima Y, Mita S. Binding properties of SA4503, a novel and selective σ_1 receptor agonist. *Eur J Pharmacol* 1996; 306: 271–279.
29. Fujimura K, Matsumoto J, Niwa M, Kobayashi T, Kawashima Y, In Y, et al. Synthesis, structure and quantitative structure-activity relationships of σ receptor ligands, 1-[2-(3,4-dimethoxyphenyl)ethyl]-4-(3-phenylpropyl) piperazines. *Bioorg Med Chem* 1997; 5: 1675–1683.
30. Mishina M, Ishiwata K, Ishii K, Kitamura S, Kimura Y, Kawamura K, et al. Function of sigma$_1$ receptors in Parkinson's disease. *Acta Neurol Scand* 2005; 112: 103–107.
31. Elsinga PH, Kawamura K, Kobayashi T, Tsukada H, Senda M, Vaalburg W, et al. Synthesis and evaluation of [^{18}F]fluoroethyl SA4503 as a PET ligand for the sigma receptor. *Synapse* 2002; 43: 259–267.
32. Elsinga PH, Tsukada H, Harada N, Kakiuchi T, Kawamura K, Vaalburg W, et al. Evaluation of [^{18}F]fluorinated sigma receptor ligands in the conscious monkey brain. *Synapse* 2004; 52: 29–37.
33. van Waarde A, Buursma AR, Hospers GAP, Kawamura K, Kobayashi T, Ishii K, et al. Tumor imaging with two sigma receptor ligands, [^{18}F]FE-SA5845 and [^{11}C]SA4503: a feasibility study. *J Nucl Med* 2004; 45: 1939–1945.
34. Kubota K, Ishiwata K, Kubota R, Yamada S, Takahashi J, Abe Y, et al. Feasibility of fluorine-18-fluorophenylalanine for tumor imaging compared with carbon-11-L-methionine. *J Nucl Med* 1996; 37: 320–325.
35. Ono M, Hirata A, Kometani T, Miyagawa M, Ueda S, Kinoshita H, et al. Sensitivity to gefitinib ('Iressa', ZD1839) in non-small cell lung cancer cell lines correlates with dependence on the epidermal growth factor (EGF) receptor/extra cellular signal-regulated kinase 1/2 and EGF receptor/Akt pathway for proliferation. *Mol Cancer Ther* 2004; 3: 465–472.
36. Ishiwata K, Kawamura K, Wang WF, Furumoto S, Kubota K, Pascali C, et al. Evaluation of *O*-[^{11}C]methyl-L-tyrosine and *O*-[^{18}F]fluoromethyl-L-tyrosine as tumor imaging tracers by PET. *Nucl Med Biol* 2004; 31: 191–198.
37. Moody TW, Leyton J, John C. Sigma ligands inhibit the growth of small cell lung cancer cells. *Life Sci* 2000; 66: 1979–1986.
38. Leitner ML, Hohmann AG, Patrick SL, Walker JM. Regional variation in the ratio of sigma$_1$ to sigma$_2$ binding in rat brain. *Eur J Pharmacol* 1994; 259: 65–69.
39. Waterhouse RN, Collier TL. *In vivo* evaluation of [^{18}F]1-(3-fluoropropyl)-4-(4-cyanophenoxymethyl)piperidine: a selective sigma-1 receptor radioligand for PET. *Nucl Med Biol* 1997; 24: 127–134.
40. Georg A, Friedl A. Characterization of specific binding sites for [^{3}H]-1,3-di-*o*-tolyl-guanidine (DTG) in the rat glioma cell line C6-BU-1. *Glia* 1992; 6: 258–263.
41. Shiue C, Shiue GG, Benard F, Visonneau S, Santoli D, Alavi AA. *N*-(*N*-Benzylpiperidin-4-yl)-2-[^{18}F]fluorobenzamide: a potential ligand for PET imaging of breast cancer. *Nucl Med Biol* 2000; 27: 763–767.
42. John CS, Vilner BJ, Schwartz AM, Bowen WD. Characterization of sigma receptor binding sites in human biopsied solid breast tumors. *J Nucl Med* 1996; 37 (Suppl): 267P (abstract).